The Schwarzschild black hole as a gravitational mirror

W. M. Stuckey

Citation: American Journal of Physics **61**, 448 (1993); doi: 10.1119/1.17434
View online: https://doi.org/10.1119/1.17434
View Table of Contents: https://aapt.scitation.org/toc/ajp/61/5
Published by the American Association of Physics Teachers

The Schwarzschild black hole as a gravitational mirror

W. M. Stuckey
Department of Physics, Elizabethtown College, Elizabethtown, Pennsylvania 17022

(Received 22 June 1922; accepted 27 September 1992)

The gravitational field outside of a nonrotating black hole is described using the Schwarzschild metric. The geodesic equations of the Schwarzschild metric are derived and those describing null and circular timelike orbits are discussed. Some numerical solutions of the null geodesic equations are shown. These depict photon trajectories which circle the black hole one or two times and then terminate at their emission points. Thus a sequence of ring-shaped mirror images is produced. An equation which gives the angle between the photon's trajectory and the radial direction at the emitter is derived and applied to the numerical solutions. These results serve to illustrate how an observer "passes through" his or her mirror image at $r=3\,MG/c^2$, as he or she moves toward a Schwarzschild black hole.

I. INTRODUCTION

Black holes and gravitational lensing are often described in introductory and popularized astronomy literature. However, these sources rarely mention that lensing due to black holes can be so severe as to send photons back to their source,[1] thus producing a "gravitational mirror." This paper in part explains the gravitational mirror effect created by a nonrotating black hole, i.e., a Schwarzschild black hole. The paper in full is intended to complement papers by Schastok *et al.*[2] and Ohanian[3] on black hole lensing which previously appeared in this journal.

It is assumed the reader has completed only the first 2 years of a typical undergraduate physics curriculum. Thus we begin in Secs. II and III with a brief introduction to black holes, gravitational lensing, general relativity (GR), the metric, and the geodesic. The reader already familiar with these topics can skip Secs. II and III without loss of continuity.

Section IV contains an explanation of the Schwarzschild metric. Radial and temporal measurements made in the Schwarzschild gravitational field are discussed. The GR origins of the terms "event horizon," "Schwarzschild radius," and "black hole" are given therein.

The geodesic equations for the Schwarzschild metric are derived in Sec. V. These equations are then applied to the cases of circular timelike and null geodesics of the Schwarzschild field. Some numerical solutions of the null geodesic equations are shown and a qualitative description of the photon motion is given.

Section VI begins with a derivation of the equation for the angle between a light ray (photon spatial trajectory) and the radial direction, as measured by an observer at rest with respect to the black hole. We apply this equation to the eight numerical solutions obtained at four spatial locations. These results illustrate how an observer "passes through" his or her mirror image as he or she approaches the black hole.

The paper concludes with an appendix outlining the numerical analysis employed herein. The method and choice of step size are described.

II. BLACK HOLES AND GRAVITATIONAL LENSING

The Newtonian version of a black hole was first introduced in the late 1700s and is not related to its relativistic counterpart.[4] The Newtonian black hole is a massive body with an escape velocity from its surface exceeding the speed of light. Since light cannot escape (to infinity) from its surface, the body is black when viewed from a large enough distance.

The modern concept of a black hole is obtained from Einstein's theory of general relativity. As with the Newtonian black hole, the GR black hole owes its name to the fact that it is a region of space from which not even light can escape. Because black holes are not directly observable, astronomers collect data which can only infer the existence of black holes.

For example, recent discoveries suggest the presence of large black holes in some galactic nuclei.[5] Specifically astronomers have found a cosmic jet (a stream of ionized matter thousands of light years long emanating from the nucleus of a galaxy) associated with M87, a giant elliptical galaxy in the Virgo cluster. Observations of the nucleus of M87 also reveal a tremendously dense concentration of stars rotating about its center with large orbital speeds. Based on these observations, many astronomers believe an enormous black hole resides in M87's nucleus. This black hole, perhaps five billion times more massive than the Sun, would form M87's cosmic jet as it consumed stars.[6] Its exceptionally strong gravitational field would provide the centripetal acceleration needed to explain the high orbital speeds of the stars in M87's nucleus.

Astronomers have somewhat more compelling evidence that smaller black holes, of only a few solar masses, reside in our galaxy.[7] These black hole candidates are x-ray sources in orbits about normal stars. The three most promising candidates are Cygnus X-1, A0620-00, and V404 Cygni. Their masses and sizes are inferred by their orbital characteristics. Given their masses and sizes, the objects must be black holes according to current theories of stellar evolution. Astronomers believe these black holes emit x-rays as they accrete material from their binary companions. Black holes existing in relative isolation, which therefore do not accrete matter, will be much more difficult to find. Some astronomers believe that gravitational lensing will produce evidence for the existence of these isolated black holes.[8]

Simply put, gravitational lensing is the "bending" of light rays in a gravitational field. The "bent" light rays produce a distorted image of the emitter.[9] Astronomers believe they have observed gravitational lensing between

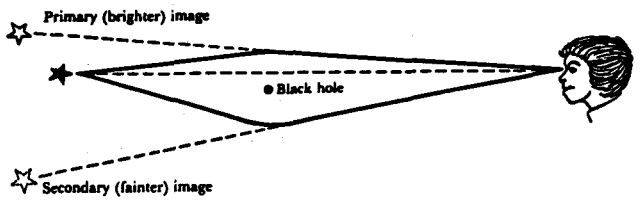

Fig. 1. An observer sees multiple images (here showing just two) of a distant object when light is "bent" around a black hole. [From Universe, by Wm. J. Kaufmann III. Copyright (c) 1985 by W. H. Freeman and Company. Reprinted by permission.]

extragalactic objects,[10] but they are not yet convinced that they have observed lensing by and between galactic objects.[11]

Because gravitational lensing produces a distorted image, it may serve as a tool for locating isolated black holes. If Earth is closely aligned with a distant star and an intervening black hole, gravitational lensing will produce multiple images of the distant star (Fig. 1). Thus Paczynski and Alcock are establishing searches which will utilize "close alignment lensing" to search for black holes and other dark bodies in our galaxy.[12] (An isolated black hole which is not "closely aligned" with Earth and a distant star will still produce multiple images of every source in the sky, but these images are probably too faint to be detected.[13])

To understand how a black hole or any massive object lenses light, one must be familiar with GR. To understand GR, it helps to be familiar with the geometry of curved spaces. Therefore these concepts are introduced in the following section.

III. GENERAL RELATIVITY AND GEOMETRY

Recall that in special relativity (SR) all inertial frames move at constant velocities relative to one another. This aspect of SR is generalized in GR so that it is possible to have inertial frames accelerating relative to one another. In order to have inertial frames accelerate relative to one another, spacetime must be curved. The world lines of inertial observers, those in free fall (or "free float" as Wheeler[14] describes it), are then "straight lines" or geodesics of the curved spacetime. (This concept of a "geodesic" will be explained later in this section.)

Spacetime becomes curved with the introduction of mass-energy. (SR relates mass and energy via $E=mc^2$.) Einstein's equations of GR relate the mass-energy-momentum content of spacetime to its resulting curvature. As described in *Gravitation*,[15] there is an "action of geometry on matter and the reaction of matter on geometry." Therefore GR is a theory of gravity. A key to understanding the structure of curved spacetime is a tensor called the metric. One solves Einstein's equations of GR to obtain the metric, and it serves as a tool for understanding the gravitational field.

A simple understanding of the metric is obtained from its role as ds^2, the infinitesimal distance squared in the spacetime. According to SR, the distance along a world line is proportional to the proper time elapsed for an observer moving on that world line. Thus

$$ds^2=-c^2d\tau^2, \tag{1}$$

where c is the speed of light in vacuum and τ is the proper time measured by the world line traveler. (The minus sign arises because we are in spacetime, rather than just space, and the inner product of a timelike vector with itself is negative.) For photons, which travel on null world lines, $ds^2=0$.

As an example in space, consider ds^2 in $\mathscr{R}^2$. Using Cartesian coordinates the infinitesimal distance squared (or simply, "the metric") is

$$ds^2=dx^2+dy^2. \tag{2}$$

Denoting the coordinates x as x^1 and y as x^2 (not to be confused with "x squared"), Eq. (2) can be written

$$ds^2=(dx^1)^2+(dx^2)^2=\sum_{i=1}^{2}\sum_{j=1}^{2} g_{ij}dx^i\,dx^j, \tag{3}$$

where

$$g_{ij}=\begin{pmatrix}1 & 0\\ 0 & 1\end{pmatrix}, \tag{4}$$

or $g_{11}=1$, $g_{12}=0$, $g_{21}=0$, and $g_{22}=1$.

If one is using polar coordinates in $\mathscr{R}^2$, the metric is

$$ds^2=dr^2+r^2d\theta^2. \tag{5}$$

Denoting the coordinates r as x^1 and θ as x^2, the metric's matrix representation is

$$g_{ij}=\begin{pmatrix}1 & 0\\ 0 & r^2\end{pmatrix}, \tag{6}$$

or $g_{11}=1$, $g_{12}=0$, $g_{21}=0$, and $g_{22}=r^2$.

Metrics in spacetimes (rather than just space) are usually written with Greek indices (rather than Latin) and use x^0 as the time coordinate. Also,

$$ds^2=\sum_{\alpha=0}^{3}\sum_{\beta=0}^{3} g_{\alpha\beta}dx^\alpha\,dx^\beta, \tag{7}$$

is usually shortened by omitting the summation signs—the repeated upper and lower indices implying a sum over all spacetime dimensions. This is called the Einstein summation convention. Both of these conventions will be used in this paper which continues now with an explanation of the geodesic.

A geodesic is a curve of extremum length between two spacetime points (label them S and T). Since the notion of length is described infinitesimally by the metric, we have naturally

$$\begin{aligned}L&=\int_S^T \sqrt{-ds^2}\\ &=\int_S^T \sqrt{-g_{\alpha\beta}dx^\alpha\,dx^\beta}\\ &=\int_S^T \sqrt{-g_{\alpha\beta}\frac{dx^\alpha}{dp}\frac{dx^\beta}{dp}}\,dp,\end{aligned} \tag{8}$$

as the length of a curve between points S and T as described by the coordinate functions $x^\mu(p)$. [The minus sign is introduced in spacetime since, as shown in Eq. (1), a timelike ds^2 is negative.] In calculus when you want to find the extremum of a function $f(x)$, you find those values of x where $df/dx=0$. An analogous situation holds for finding geodesics of the spacetime. One finds the curve between

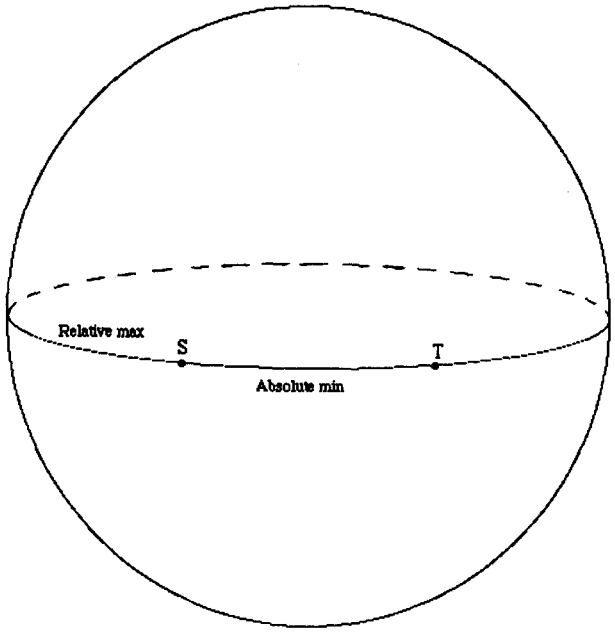

Fig. 2. The segments of the equator connecting points S and T of a sphere are geodesics.

points S and T specified by $\{x^\mu(p)\}$, such that $\delta L=0$ for arbitrary $\delta x^\mu(p)$. Then curves nearby this geodesic, given by $\{x^\mu(p)+\delta x^\mu(p)\}$, are slightly longer or shorter curves than the geodesic.

For example, consider the points S and T on the equator of a sphere as shown in Fig. 2. The curve of absolute minimum length is the short segment of the equator between points S and T. Therefore this piece of the equator is a geodesic between S and T. Now consider the long segment of the equator between S and T. The length of this curve is a relative maximum, since nearby curves are a little shorter. Therefore, it too is a geodesic between S and T.

Demanding that $\delta L=0$ for all $\delta x^\mu(p)$ gives[16]

$$\frac{d^2x^\mu}{dp^2}+\Gamma^\mu_{\alpha\beta}\frac{dx^\alpha}{dp}\frac{dx^\beta}{dp}=0, \tag{9}$$

where

$$\Gamma^\mu_{\alpha\beta}=\frac{g^{\mu\eta}}{2}\left(\frac{\partial g_{\eta\alpha}}{\partial x^\beta}+\frac{\partial g_{\eta\beta}}{\partial x^\alpha}-\frac{\partial g_{\alpha\beta}}{\partial x^\eta}\right), \tag{10}$$

is called the Christoffel symbol of the second kind. (Hereafter, it is referred to as simply the "Christoffel symbol.") The $g^{\mu\eta}$ are the elements of the metric's inverse matrix. For example, the $g^{\mu\eta}$ for Eq. (6) would be

$$g^{\mu\eta}=\begin{pmatrix}1 & 0\\ 0 & 1/r^2\end{pmatrix}. \tag{11}$$

Notice there are N, second order differential equations to be solved for the N coordinate functions $x^\mu(p)$ in an N-dimensional spacetime.

For example, consider again the space $\mathscr{R}^2$ with Cartesian coordinates. All the Christoffel symbols are zero and the two differential equations to be solved are

$$\frac{d^2x}{dp^2}=0, \tag{12}$$

and

$$\frac{d^2y}{dp^2}=0. \tag{13}$$

The $x^\mu(p)$ which satisfy these differential equations are simply

$$x(p)=c_1p+c_2 \tag{14}$$

and

$$y(p)=c_3p+c_4, \tag{15}$$

where the c_i are arbitrary constants. Eliminating the parameter p and combining the arbitrary constants results in the more familiar form,

$$y(x)=mx+b, \tag{16}$$

where $m=c_3/c_1$ and $b=(c_1c_4-c_2c_3)/c_1$.

Using polar coordinates in $\mathscr{R}^2$ yields

$$\Gamma^2_{12}=\Gamma^2_{21}=\frac{1}{r} \tag{17}$$

and

$$\Gamma^1_{22}=-r, \tag{18}$$

for the nonzero Christoffel symbols. The geodesic equations are then

$$\frac{d^2r}{dp^2}+-r\left(\frac{d\theta}{dp}\right)\left(\frac{d\theta}{dp}\right)=0 \tag{19}$$

and

$$\frac{d^2\theta}{dp^2}+\frac{2}{r}\left(\frac{d\theta}{dp}\right)\left(\frac{dr}{dp}\right)=0. \tag{20}$$

One solution of these equations is

$$r=c_1p+c_2 \tag{21}$$

and

$$\theta=c_3, \tag{22}$$

where the c_i are arbitrary constants. This is the family of straight lines through the origin, a subset of Eq. (16). Of course the set of all solutions to Eqs. (19) and (20) must be equal to Eq. (16), i.e., straight lines written in polar coordinates.[17]

This section has offered only a brief introduction to GR, the metric, and the geodesic. However, it does provide a sufficient basis for understanding the calculations presented in Secs. IV and V.

IV. THE SCHWARZSCHILD GEOMETRY

Solving Einstein's equations of GR for the metric outside a spherically symmetric, static (does not change with time) body of total mass-energy M yields[18]

$$ds^2=-c^2\left(1-\frac{2GM}{c^2r}\right)dt^2+\left(1-\frac{2GM}{c^2r}\right)^{-1}dr^2+r^2d\theta^2 +r^2(\sin^2\theta)d\varphi^2. \tag{23}$$

The geometry (or gravitational field) described by this metric is called the *Schwarzschild geometry* after the man who derived the solution in 1916, Karl Schwarzschild. In this metric, G is Newton's gravitational constant, θ and φ

are the polar and azimuthal coordinates, t is the coordinate time, and r is the radial coordinate. Because the body producing this geometry is spherically symmetric, the radial component of $g_{\alpha\beta}$ is the only spatial component differing from its Euclidean counterpart. Because the body producing this geometry is static, the $g_{\alpha\beta}$ are not functions of time.

The radial coordinate of this metric is defined via area measurements around the body. Given the area A of a hypothetical spherical surface (all points of which lie equal distance from the body), the radial coordinate of the points on this surface is defined as

$$r:=\sqrt{A/4\pi}. \tag{24}$$

Therefore, the radial coordinate of a hypothetical circle on this sphere in the $\theta=\pi/2$ plane is

$$r\equiv C/2\pi, \tag{25}$$

where C is the circumference of the circle. Of course this is also the result in $\mathscr{R}^2$. However in $\mathscr{R}^2$ the radial distance between concentric circles of radii R_2 and R_1 is

$$\Delta s=\int_{R_1}^{R_2} dr=R_2-R_1, \tag{26}$$

whereas in the Schwarzschild geometry the radial distance between such circles is

$$\begin{aligned}\Delta s&=\int_{R_1}^{R_2}\frac{dr}{\sqrt{1-\dfrac{2M}{r}}}\\&=R_2\sqrt{1-\frac{2M}{R_2}}-R_1\sqrt{1-\frac{2M}{R_1}}\\&\quad+(2M)\ln\left(\frac{\sqrt{R_2}+\sqrt{R_2-2M}}{\sqrt{R_1}+\sqrt{R_1-2M}}\right)\end{aligned} \tag{27}$$

(Here and throughout the remainder of the paper M denotes GM/c^2.) The result of Eq. (27) is larger than the result of Eq. (26). Therefore, the radial distance between concentric circles in the Schwarzschild geometry is greater than the radial distance between circles of like circumferences in Euclidean geometry (see Fig. 3).

For example, consider the two concentric circles of radii $R_2=2$ m and $R_1=1$ m in a spacetime with negligible mass-energy content, i.e., a flat spacetime. The circumferences of these two circles are 4π m and 2π m, respectively, and the radial distance between the circles is simply 2 m$-$1 m$=$1 m. Now at the coordinate origin place a small (with respect to volume) mass $M_{\rm E}$ equal to that of the Earth's (5.98×10^{24} kg). The "equatorial" circle about this mass with circumference 4π m has radial coordinate $R_2=2$ m by definition. Likewise the "equatorial" circle about this mass with circumference 2π m has radial coordinate $R_1=1$ m. Equation (27) then gives the radial distance between these circles as 1.0031 m.

Replace $M_{\rm E}$ with an object of one solar mass ($M_{\rm Sun}$) and Eq. (27) yields imaginary results for $R_i<3$ km. In fact at $r=2GM_{\rm Sun}/c^2$, the Schwarzschild metric is singular. In general the singularity arising at $r=2$ M is denoted R_S and called the *Schwarzschild radius.* The other value at which the Schwarzschild metric is singular is $r=0$. The R_S singularity is a coordinate singularity, i.e., it disappears under an appropriate coordinate transformation.[19] No signals from spacetime events with $r<R_S$ can reach observers at

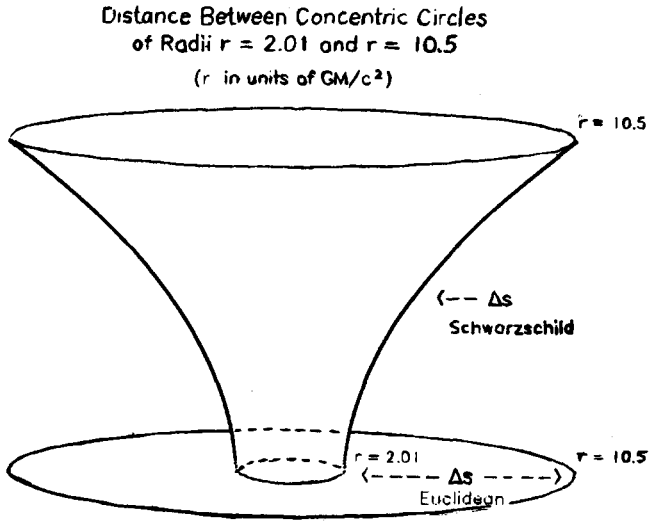

Fig. 3. The radial distances between two concentric circles in the Schwarzschild metric and the Euclidean metric are contrasted. Notice that the radial distance between these circles is greater in the Schwarzschild metric (distance along the curve labeled "Δs Schwarzschild"), even though the circumference of the circles are the same in both geometries.

$r>R_S$. Thus the name *event horizon* is given to the Schwarzschild radius. The $M_{\rm Sun}$ black hole has a Schwarzschild radius of 3 km. Since nothing (not even light) can escape this region, it is called a *Schwarzschild black hole.*

(Herein lies the difference alluded to in Sec. II between the Newtonian black hole and the relativistic black hole. According to Newtonian physics if a body has a density such that the escape velocity from its surface is c, light is not confined to the surface. Rather the velocity of the emitted photons goes to zero as the light goes to infinity. Therefore this body does not appear black, except to those observers at infinity. The relativistic black hole on the other hand, appears black to observers at all $r>R_S$.)

If an object is compressed into its $r<R_S$ region, then no known force can stop it from self-gravitating to infinite density at $r=0$. Therefore the $r=0$ singularity is a physical singularity, i.e., a place where the known laws of physics can no longer describe nature.

Again the Schwarzschild metric is only valid outside the body, so these singular radii are only relevant when the body in question is a black hole. The following calculations deal predominately with the space outside of black holes, so it should be noted that Eq. (27) can be applied at $R_1=R_S$. Thus the definition of the radial coordinate can be modified to read, "...(all points which lie equal distance from the event horizon)..." for use about a black hole.

Having introduced the spatial curvature, we turn now to the temporal curvature. Coordinate time of the Schwarzschild geometry is the proper time measured by observers at rest ($dr=d\theta=d\varphi=0$) at $r=\infty$. The metric relates proper time elapsed for observers at rest at finite r to the passage of coordinate time via

$$ds^2=-c^2d\tau^2=-c^2\left(1-\frac{2M}{r}\right)dt^2 \tag{28}$$

so that

$$\Delta\tau=\sqrt{1-\frac{2\ \mathrm{M}}{r}}\,\Delta t. \tag{29}$$

Thus an observer near the black hole ages more slowly than observers farther from the black hole.

This is a small effect about objects with masses and volumes comparable to Earth's. An expansion of $\sqrt{1-2\ \mathrm{M}/r}$ in Eq. (29) to first order in $2\ \mathrm{M}/r$ yields $\Delta\tau\cong(1-\mathrm{M}/r)\Delta t$. Using the mass and radius of the Earth, you find that $(1-\Delta\tau/\Delta t)$ is a mere 7×10^{-10}.

In closing this section, it should be noted that the Schwarzschild metric reduces to the flat spacetime metric in spherical coordinates, as r goes to infinity. That is to say, the gravitational field is negligible far from the source. The following equations explain the geodesic motion of photons (or any massless particle), as well as circular time-like geodesic motion, throughout the $r>R_S$ region.

V. GEODESICS OF THE SCHWARZSCHILD GEOMETRY

The calculations of this section deal exclusively with motion in the $\theta=\pi/2$ plane without loss of generality. This is because spherical symmetry requires planar geodesics. The plane of any given geodesic can then, via a judicious choice of coordinate assignment, be described by $\theta=\pi/2$. Thus we are concerned with motion for which

$$ds^2=-c^2\left(1-\frac{2\ \mathrm{M}}{r}\right)dt^2+\left(1-\frac{2\ \mathrm{M}}{r}\right)^{-1}dr^2+r^2d\varphi^2. \tag{30}$$

Assign $x^0=t$, $x^1=r$, and $x^2=\varphi$ and the nonzero Christoffel symbols are

$$\Gamma^1_{11}=\Gamma^0_{10}=\Gamma^0_{01}=\frac{\mathrm{M}}{r^2\left(1-\frac{2\ \mathrm{M}}{r}\right)},\quad \Gamma^1_{00}=\frac{c^2\mathrm{M}}{r^2}\left(1-\frac{2\ \mathrm{M}}{r}\right),$$
$$\Gamma^1_{22}=-r\left(1-\frac{2\ \mathrm{M}}{r}\right),\quad \Gamma^2_{21}=\Gamma^2_{12}=\frac{1}{r}. \tag{31}$$

Equation (9) then gives the three geodesic equations of the Schwarzschild geometry as

$$\frac{d^2t}{dp^2}+2\Gamma^0_{10}\left(\frac{dt}{dp}\right)\left(\frac{dr}{dp}\right)=0, \tag{32}$$

$$\frac{d^2r}{dp^2}+\Gamma^1_{00}\left(\frac{dt}{dp}\right)^2+\Gamma^1_{11}\left(\frac{dr}{dp}\right)^2+\Gamma^1_{22}\left(\frac{d\varphi}{dp}\right)^2=0, \tag{33}$$

$$\frac{d^2\varphi}{dp^2}+2\Gamma^2_{21}\left(\frac{d\varphi}{dp}\right)\left(\frac{dr}{dp}\right)=0. \tag{34}$$

That these admit circular, timelike geodesic orbits about the black hole can be shown as follows.

For timelike ($p=\tau$) curves with $r=r_0$ (a constant), Eqs. (32)–(34) give

$$\frac{d^2t}{d\tau^2}=0, \tag{35}$$

$$\Gamma^1_{00}\left(\frac{dt}{d\tau}\right)^2+\Gamma^1_{22}\left(\frac{d\varphi}{d\tau}\right)^2=0, \tag{36}$$

$$\frac{d^2\varphi}{d\tau^2}=0. \tag{37}$$

The solutions of Eqs. (35) and (37) are simply

$$t=c_1\tau+c_2 \tag{38}$$

and

$$\varphi=c_3\tau+c_4, \tag{39}$$

where the c_i are arbitrary constants. Equation (36) gives (for $r_0>R_S$)

$$\frac{d\varphi}{dt}=\pm c\sqrt{\mathrm{M}/(r_0)^3} \tag{40}$$

(which is equivalent to the Newtonian result when $t\cong\tau$, i.e., the gravitational field is weak). Thus there are circular timelike geodesics in the Schwarzschild geometry given by $r=r_0$, $\varphi=c_3\tau+c_4$, and $t=c_1\tau+c_2$, where the c_i are arbitrary constants except that $c_3/c_1=\sqrt{\mathrm{M}/(r_0)^3}$.

Proper time elapsed versus coordinate time elapsed for circular geodesic travelers is then given by Eqs. (8) and (30) as

$$\Delta\tau=\frac{1}{c}\int\sqrt{-g_{\alpha\beta}dx^\alpha dx^\beta}$$
$$=\frac{1}{c}\int\sqrt{c^2\left(1-\frac{2\ \mathrm{M}}{r_0}\right)dt^2-(r_0)^2d\varphi^2}. \tag{41}$$

Using Eq. (40) and the chain rule for dt yields

$$\Delta\tau=\frac{1}{c}\int\sqrt{c^2\left(1-\frac{2\ \mathrm{M}}{r_0}\right)-\frac{c^2\ \mathrm{M}}{r_0}}\,dt=\sqrt{1-\frac{3\ \mathrm{M}}{r_0}}\,\Delta t. \tag{42}$$

Notice $\Delta\tau=0$ for $r_0=3$ M, i.e., $r_0=3$ M is a null circular geodesic. Thus photons have a circular orbit about the black hole at $r_0=3$ M. This orbit is called the *photon circle* or *photon sphere*.[20] The following investigation of null geodesics will also obtain this result.

For null geodesics ($ds^2=0$), Eq. (30) gives

$$c^2\left(1-\frac{2\ \mathrm{M}}{r}\right)dt^2=\left(1-\frac{2\ \mathrm{M}}{r}\right)^{-1}dr^2+r^2d\varphi^2. \tag{43}$$

This can be rewritten using two conserved quantities obtained via the geodesic equations. These conserved quantities exist for geodesic motion, because the spacetime has two symmetries, i.e., it's spherically symmetric and static.

Equation (34) can be rewritten as

$$d\left(r^2\frac{d\varphi}{dp}\right)\Big/dp=0, \tag{44}$$

thus

$$r^2\frac{d\varphi}{dp}=\text{constant}:=L. \tag{45}$$

In the case of timelike orbits ($p=\tau$), L is the angular momentum per unit mass.[21] Along null geodesics, we may assume that L is related to the angular momentum of the photon.[22]

Another conserved quantity is obtained from Eq. (32), which can be rewritten as

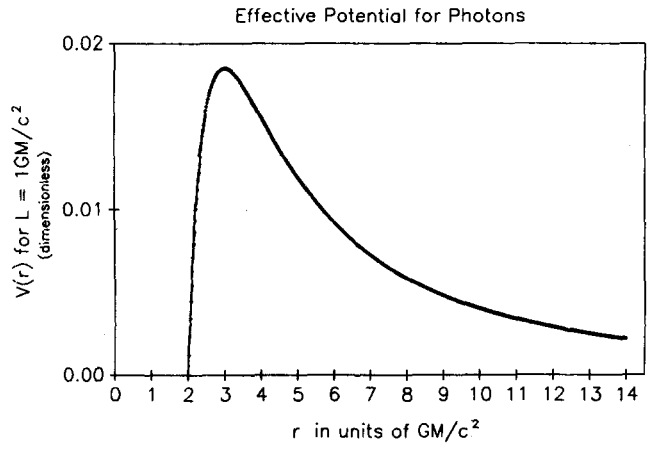

Fig. 4. A photon's radial motion can be understood qualitatively using this "effective potential."

$$d\left[\left(1-\frac{2\ \mathrm{M}}{r}\right)\left(\frac{dt}{dp}\right)\right]\Big/dp=0, \tag{46}$$

and therefore

$$\left(1-\frac{2\ \mathrm{M}}{r}\right)\left(\frac{dt}{dp}\right)=\text{constant}:=E. \tag{47}$$

In the case of timelike orbits, Ec^2 can be interpreted as the total energy (including gravitational potential energy) per unit mass of the geodesic traveler. Along null geodesics, we may assume that E is related to the total energy of the photon.[23]

Using these two conserved quantities, Eq. (43) can be rewritten as

$$c^2E^2=\left(\frac{dr}{dp}\right)^2+\frac{L^2}{r^2}\left(1-\frac{2\ \mathrm{M}}{r}\right). \tag{48}$$

This equation has the form of a unit-mass particle of total energy $c^2E^2/2$ moving in a one-dimensional "effective potential" given by

$$V(r)=\frac{L^2}{2r^2}\left(1-\frac{2\ \mathrm{M}}{r}\right). \tag{49}$$

Figure 4 displays this potential. To find the maximum of $V(r)$ one must solve

$$\frac{dV}{dr}=\frac{-L^2}{r^3}\left(1-\frac{2\ \mathrm{M}}{r}\right)+\frac{L^2\ \mathrm{M}}{r^4}=0. \tag{50}$$

The solution is $r_{\max}=3$ M, independent of L. This is the circular orbit found previously for photons. Because this orbit is a maximum of $V(r)$, it is an unstable orbit, i.e., a slight deviation from this orbit sends the photon into the black hole or to infinity. Further study of $V(r)$ allows for some qualitative understanding of photon motion in the Schwarzschild geometry.

First, consider photons emitted from $r>3$ M. If emitted with $dr/dp>0$, i.e., away from the black hole, the photon simply proceeds to infinity. If $dr/dp<0$, there are three possible results. If E is such that $c^2E^2/2=V(r=r_{\max})$, then the photon ends up in the unstable circular orbit at $r=3$ M. (Assign E_c to this value of E.) If $E>E_c$, then dr/dp never increases to zero and the photon proceeds into the black hole. If $E<E_c$, then the photon reaches a minimum value of $r(r_m)>3$ M where according to Eq. (48), $dr/dp=0$. Thereafter dr/dp is greater than zero and the photon proceeds to infinity. In this case, it is possible that the photon returns to its emitter (Fig. 5). This will be discussed in Sec. VI.

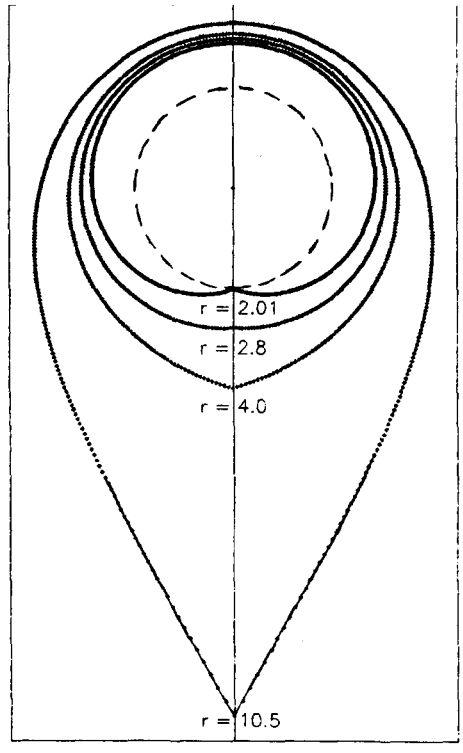

Fig. 5. Numerical solutions showing "boomerang photons" emitted from inside and outside the photon circle about a black hole. The event horizon is shown with the dashed curve. The values of r_0 are given in units of GM/c^2. The emission angles are 10.53° at $r_0=2.01$, 82.75° at $r_0=2.8$, 66.83° at $r_0=4.0$, and 26.74° at $r_0=10.5$.

Consider now photons emitted from $r<3$ M. If emitted with $dr/dp<0$, i.e., toward the black hole, the photon simply proceeds into the black hole. If $dr/dp>0$, there are three possible results. If $E=E_c$, then the photon ends up in the circular orbit at $r=3$ M. If $E>E_c$, then dr/dp never decreases to zero and the photon proceeds to infinity. If $E<E_c$, the photon reaches a maximum value of $r(r_m)<3$ M where according to Eq. (48), $dr/dp=0$. Thereafter dr/dp is less than zero and the photon proceeds into the black hole. Again in this case, the photon may return to its emitter (Fig. 5). (See also the discussion given in Ref. 24.)

VI. BOOMERANG EMISSION

Among the aforementioned scenarios, consider those cases where dr/dp changes sign and the photon returns to its emitter. As r_m approaches 3 M, the photon undergoes a larger angular displacement before dr/dp changes sign. Thus the photon may circumnavigate the black hole one (Fig. 5), two (Figs. 6–9), or more times before returning to its emitter.

The angle of photon emission with respect to the radial direction (δ) determines r_m. For the emitter there is rota-

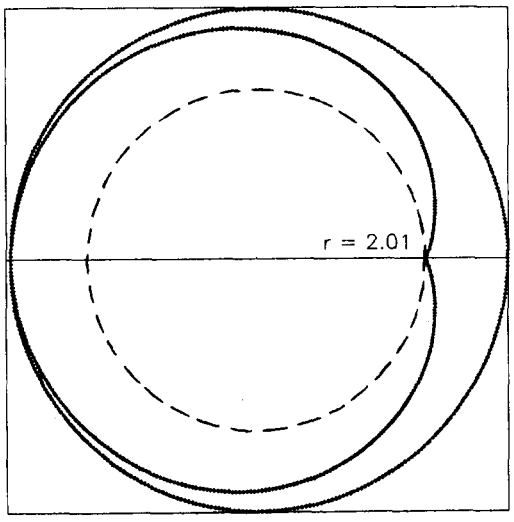

Fig. 6. The numerical solution of a "boomerang photon" emitted from very near (r_0=2.01 GM/c^2) the event horizon (dashed curve) of a black hole. The emission angle (10.50627°) is such that the photon made two orbits of the black hole before returning to its emitter. The border is tangent to the photon circle.

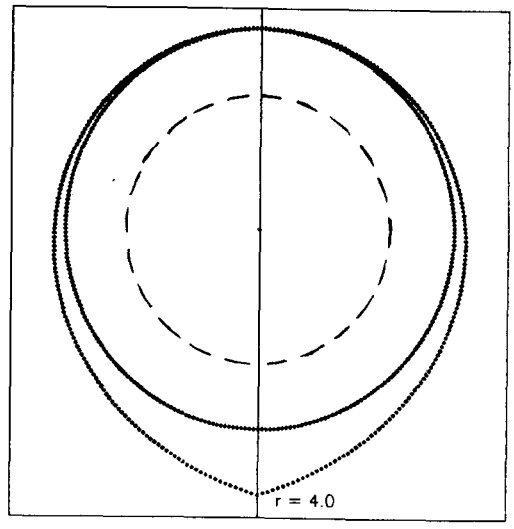

Fig. 8. The numerical solution of a "boomerang photon" emitted from a position near and outside (r_0=4.0 GM/c^2) the photon circle of a black hole (event horizon shown with dashed curve). The emission angle (66.71648°) is such that the photon made two orbits of the black hole before returning to its emitter.

tional symmetry about the radial direction and therefore the angle of emission is also the angle of reception. This angle can be obtained as follows.

Equation (43) can be rewritten to give

$$c^2=\left(1-\frac{2\ \mathrm{M}}{r}\right)^{-1}\frac{dr^2}{\left(1-\frac{2\ \mathrm{M}}{r}\right)dt^2}+r^2\frac{d\varphi^2}{\left(1-\frac{2\ \mathrm{M}}{r}\right)dt^2}. \tag{51}$$

However, Eq. (28) gives $(1-2\ \mathrm{M}/r)dt^2=d\tau^2$ for the observer at rest at r. Thus we have

$$c^2=\left(1-\frac{2\ \mathrm{M}}{r}\right)^{-1}\left(\frac{dr}{d\tau}\right)^2+r^2\left(\frac{d\varphi}{d\tau}\right)^2, \tag{52}$$

for the square of the photon's speed as measured by an observer at rest at r (here assumed to be the emitter). The terms on the right-hand side of Eq. (52) can be identified as the radial and angular components of c^2. Therefore the emitter at r_0 measures an angle between the photon's trajectory and the radial direction of

$$\delta=\arctan\left(\sqrt{1-\frac{2\ \mathrm{M}}{r_0}}\,r_0\frac{d\varphi}{dr}\right). \tag{53}$$

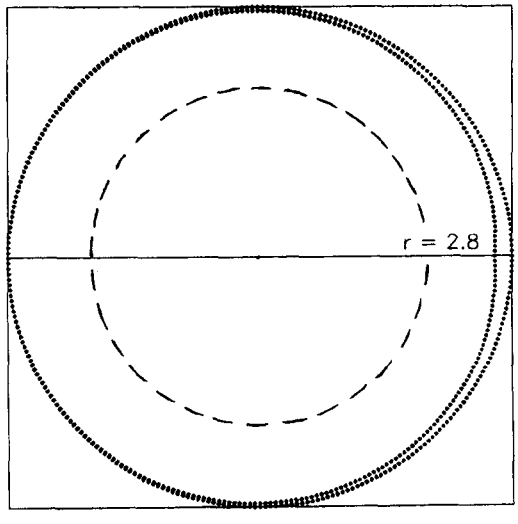

Fig. 7. The numerical solution of a "boomerang photon" emitted from a position near and inside (r_0=2.8 GM/c^2) the photon circle of a black hole (event horizon shown with dashed curve). The emission angle (82.72519°) is such that the photon made two orbits of the black hole before returning to its emitter. The border is tangent to the photon circle.

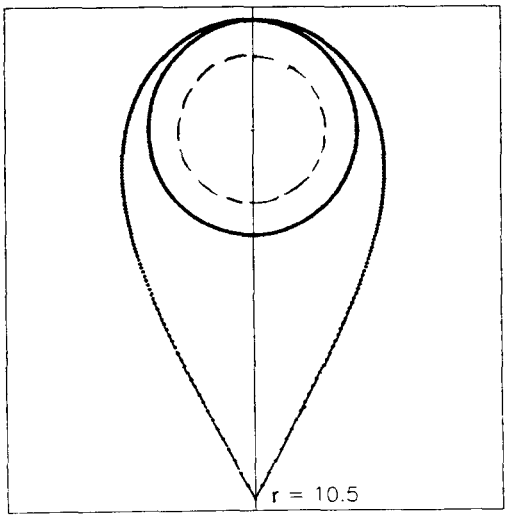

Fig. 9. The numerical solution of a "boomerang" photon emitted from a position outside (r_0=10.5 GM/c^2) the photon circle of a black hole (event horizon shown with dashed curve). The emission angle (26.44011°) is such that the photon made two orbits of the black hole before returning to its emitter.

(The ± signs coming from square roots are omitted in all arctan functions with the understanding that we are concerned only with photons emitted toward $r=3$ M.) Equations (45) and (48) can be combined to give

$$\frac{d\varphi}{dr}=\pm\left(r_0\sqrt{\frac{r_0^2}{b^2}-1+\frac{2\ \mathrm{M}}{r_0}}\right)^{-1}, \tag{54}$$

where $b\equiv L/(cE)$ is called the *apparent impact parameter.*[25] Equations (53) and (54) then give

$$\delta=\arctan\left[\left(\frac{r_0}{\alpha b}\right)^2-1\right]^{-1/2}, \tag{55}$$

where $\alpha=\sqrt{1-2\ \mathrm{M}/r_0}$.

If $b=\sqrt{27}$ M, then $E=E_c$ according to Eq. (48) and the photon is emitted so as to be captured in the photon circle. This critical angle is given by Eq. (55) as

$$\delta_c=\arctan\left[\left(\frac{r_0}{\alpha\sqrt{27}\ \mathrm{M}}\right)^2-1\right]^{-1/2}. \tag{56}$$

For $\delta<\delta_c$, the photon is captured by the black hole ($r_0>3\ m$) or escapes to infinity ($r_0<3\ m$). Therefore we are concerned only with those emissions for which $\delta>\delta_c$.

As δ goes to δ_c, r_m goes to 3 M. As stated previously, as r_m goes to 3 M the photon makes more orbits around the black hole before returning to its emitter. Thus the "boomerang photon" which makes one orbit around the black hole is emitted at larger δ (δ_1) than the "boomerang photon" which makes two orbits (emitted at δ_2), and so on. The δ_i must therefore satisfy $\delta_c<\delta_i<\delta_1$. At $r_0=3$ M, $\delta_1=\delta_c=90°$ and so all the $\delta_i=90°$. At infinite r_0 the b_i corresponding to any δ_i is finite,[26] so Eqs. (55) and (56) give $\delta_c=\delta_i=0°$. At $r=2$ M all images are seen[27] at $\delta=0°$, thus $\delta_c=\delta_i=0°$. Using these results, we now construct the angular distribution of the mirror images seen by an observer moving (slowly) from $r_0=\infty$ to $r_0=2$ M.

Consider the observer at r_0 which emits (or reflects) light uniformly in all directions. This observer will see rings of "boomerang photons" at angles δ_i. The rings will be distributed between δ_c and δ_1, and the set of rings will have some angular extent about the radial direction. The distribution of the rings within the set, and the angular extent of the set will change as the observer changes his or her radial location.

As the observer moves from infinity, the set is seen in the direction of the black hole and its angular extent increases from zero. The distribution of the rings in the set also increases, so they appear to "fan out" from a point in the direction of the black hole. In moving toward $r_0=3$ M, the rings eventually stop spreading out and begin to converge. Meanwhile, the angular extent of the set is increasing to 90°. When the observer reaches the photon circle, all the images overlap at 90°. Thus the observer has "moved inside" his or her circular mirror image.

In continuing toward the black hole, the images appear in the direction opposite the black hole. That is, the observer has "passed through" his or her mirror image. The rings, still sandwiched between δ_c and δ_1, again "fan out" as the angular extent of the set decreases from 90°. Because the set is shrinking, the rings must eventually stop spreading out and begin to converge. As the observer approaches the event horizon, the set shrinks to a point seen in the direction opposite the black hole.

Table I. Numerical results.

r_0/M	δ_1	δ_2	δ_c	b_1/M	b_2/M
2.01	10.53°	10.50627°	10.50623°	5.207	5.196172
2.80	82.75°	82.72519°	82.72514°	5.196	5.196153
4.00	66.83°	66.71648°	66.71627°	5.200	5.196161
10.5	26.74°	26.44011°	26.43956°	5.251	5.196253

Equations (55) and (56) have been applied to eight numerical solutions of photon trajectories which terminate at their emission points (Figs. 5–9). These results are given in Table I.

In closing this section, we point out an interesting feature of the numerical results. If you use a protractor to measure δ_i at $r_0=2.01$ M in Fig. 5 or 6, you obtain $\delta_i\cong 75°$. Equation (55) gives $\delta_i\cong 11°$ (Table I). This difference is due to the projection of the light ray onto the Euclidean plane. Had the light ray been graphed on the "funnel-shaped" surface shown in Fig. 3, δ_i would have an apparent value of about 11°.

APPENDIX

The numerical results were obtained using the quartic Runge–Kutta method.[28] The differential equation solved was

$$\frac{dr}{d\varphi}=\pm r\sqrt{\frac{r^2}{b^2}-1+\frac{2\ \mathrm{M}}{r}}. \tag{57}$$

[The sign was reversed when the photon reached its turning point, $c^2E^2=2V(r)$, as explained in Sec. V.] The inputs for a run were then δ, r_0, N (the number of steps), and w (the step size in φ). In practice, the total angular displacement and N were specified and these determined w. The input of δ and r_0 determined b via Eq. (55). A "good" value of w for each value of r_0 was chosen with a simple test.

The test was based on the properties of the photon circle. A "good" value of w at each r_0 was determined to be the maximum value of w (specifying N to the nearest 100,000) for which a photon emitted at δ_c would orbit the black hole ten times without spiraling out of the photon circle. The photon's radial coordinate was output after the tenth orbit, so as to obtain an estimate of numerical error. These results are given in Table II.

Last, the number of significant figures of the δ presented in Table I should be addressed. At each r_0, the number of decimal places in δ was increased in successive attempts to get the photon to return to r_0 (label this return value r_f). This process was terminated when variations of the smallest decimal place in δ did not produce consistent variations in r_f.

Table II. Step size test results ($w=2\pi/N$).

r_0/M	N	r after $\Delta\varphi=20\pi$
2.01	800,000	2.999999999087
2.80	300,000	2.999999999103
4.00	600,000	3.000000000902
10.5	600,000	3.000000000903

With $r_0 > 3$ M for example, it was demanded that an increment (of 1) in the least significant figure of δ produce an increase in r_f. Likewise a decrement (of 1) must produce a decrease in r_f. At each r_0, decimal places were added to δ until a least significant figure was found using the prescription just described, or until we had five more significant figures than were needed for comparison with δ_c. In rounding the values of δ for presentation in Table I, at least three significant figures were omitted in all cases.

[1]Frank Shu, *The Physical Universe* (University Science Books, Mill Valley, California, 1982), pp. 137–138; E. Chaliasos, "Detection of black holes from optical phenomena," Monthly Notices of the Royal Astronomical Society **237**, pp. 653–659 (1989); George Greenstein, *Frozen Star, Of Pulsars, Black Holes, and the Fate of the Universe* (New American Library, New York, 1983), pp. 142–147.

[2]Joachim Schastok, Michael Soffel, Hanns Ruder, and Manfred Schneider, "Stellar sky as seen from the vicinity of a black hole," Am. J. Phys. **55**, 336–341 (1987).

[3]Hans C. Ohanian, "The black hole as a gravitational 'lens'," Am. J. Phys. **55**, 428–432 (1987).

[4]A. K. Raychaudhuri, "Black holes and Newtonian physics," General Relativity and Gravitation **24**, 281–283 (1992); I. Nicholson, *Gravity, Black Holes and the Universe* (Halsted, New York, 1981), pp. 115–117; Walter Sullivan, *Black Holes, The Edge of Space, The End of Time* (Anchor Press/Doubleday, New York, 1979), pp. 63–67.

[5]Fay Flam, "New strategy in the hunt for black holes," Science **255**, 536–537 (1992); R. Pease, "Black hole in M87's bright spot," Nature **355**, 399 (1992); Michael A. Seeds, *Horizons, Exploring the Universe* (Wadsworth, Belmont, CA, 1991), pp. 299–300; William K. Hartmann, *The Cosmic Voyage* (Wadsworth, Belmont, CA, 1992), pp. 398–403.

[6]Martin J. Rees, "Black holes in galactic centers," Scientific American **263**, 56–66 (1990); R. Cowen, "Astro eyes new signs of black holes," Science News **138**, 372 (1990); R. Cowen, "More on black holes," Science News **139**, 10 (1991); Alan Lightman, "Still wanted: Black holes," Discover **11**, 26–33 (1990).

[7]Joseph F. Dolan, "Placing faith in the masses?" Nature **355**, 589–590 (1992); J. Casares, P. A. Charles, and T. Naylor, "A 6.5 day periodicity in the recurrent nova V404 Cygni implying the presence of a black hole," Nature **355**, 614–617 (1992); Faye Flam, "How to find a black hole," Science **255**, 794–795 (1992); R. Cowen, "New evidence for black holes in the Milky Way," Science News **141**, 101 (1992); Ken Croswell, "The best black hole in the galaxy," Astronomy **20**, 31–37 (1992).

[8]Faye Flam, "Putting a cosmic illusion to work," Science **256**, 30–31 (1992); B. Paczynski, "Is there a black hole in the sky?" Nature **321**, 419–420 (1986).

[9]The construction of lenses which mimic gravitational lenses are described in the following papers: Vincent Icke, "Construction of gravitational lens," Am. J. Phys. **48**, 883–886 (1980); J. Higbie, "Gravitational lens," Am. J. Phys. **49**, 652–655 (1981); J. Higbie, "Galactic lens," Am. J. Phys. **51**, 860–861 (1983).

[10]Sam Flamsteed, "Probing the edge of the universe," Discover **12**, 43–47 (1991); I. Peterson, "Supernova images and luminous arcs," Science News **134**, 357 (1988); Leif J. Robinson, "Giant galactic arcs," Sky & Telescope **73**, 379 (1987); Michael Lemonick, "Quadruple bypass," Discover **10**, 22 (1989); R. Cowen, " Mystery matter: Through a lens, darkly," Science News **137**, 52 (1990); Anthony Tyson, "Mapping dark matter with gravitational lenses," Physics Today **45**, 24–32 (1992).

[11]T. Padmanabhan and S. M. Chitre, "Is gravitational lensing a local phenomenon caused by Pop III objects?" Astrophys. Lett. Commun. **25**, 255–261 (1987).

[12]R. Cowen, "Hunting planets with a gravitational lens," Science News **141**, 327 (1992).

[13]Ralph P. Lano, "The brightness of a black hole due to gravitational lensing," Astrophys. Space Sci. **159**, 125–132 (1989).

[14]J. A. Wheeler, *A Journey into Gravity and Spacetime* (W. H. Freeman, New York, 1990), p. 11.

[15]C. W. Misner, K. S. Thorne, and J. A. Wheeler, *Gravitation* (W. H. Freeman, San Francisco, 1973), p. 47.

[16]William M. Burke, *Applied Differential Geometry* (Cambridge U. P., Cambridge, 1985), pp. 375–376; Robert M. Wald, *General Relativity* (The University of Chicago, Chicago, 1984), pp. 44–45; S. Weinberg, *Gravitation and Cosmology* (Wiley, New York, 1972), pp. 76–77.

[17]A. P. Lightman, W. H. Press, R. H. Price, and S. A. Teukolsky, *Problem Book in Relativity and Gravitation* (Princeton U. P., Princeton, 1975), pp. 42–43.

[18]For an intuitive explanation see: I. R. Kenyon, *General Relativity* (Oxford, U. P., Oxford, 1990), pp. 42–45. For a technical derivation see: Misner *et al.*, p. 607; Wald, pp. 119–125; Weinberg, pp. 179–180.

[19]Misner *et al.*, pp. 822–826; Wald, pp. 148–156.

[20]William J. Kaufmann III, *Relativity and Cosmology* (Harper & Row, New York, 1977), p. 48.

[21]Misner *et al.*, pp. 655–658.

[22]Wald, p. 139.

[23]Wald, p. 139; Misner *et al.*, p. 672.

[24]Misner *et al.*, p. 674–675.

[25]Wald, p. 144.

[26]C. Darwin, "The gravity field of a particle, I," Proc. Roy. Soc. London A **249**, 180–194 (1959); C. Darwin, "The gravity field of a particle, II," Proc. Roy. Soc. London A **263**, 39–50 (1961); Misner *et al.*, pp. 678–679.

[27]Schastok *et al.*, p. 339.

[28]G. P. Weeg and G. B. Reed, *Introduction to Numerical Analysis* (Blaisdell, Waltham, Massachusetts, 1966), pp. 78–86; P. A. Stark, *Introduction to Numerical Methods* (Macmillan, Collier-Macmillan Limited, London, 1970), pp. 265–267; C. E. Froberg, *Introduction to Numerical Analysis* (Addison-Wesley, Reading, Massachusetts, 1965), pp. 244–248.

THE SOCIAL RESPONSIBILITY OF SCIENTISTS

Surely it would have been better for us all ... if we had recognized that the maintenance and improvement of our present society, which owes so much to science for its creation and for its sense of values, demand also from scientists that they play their full part in working within society to develop and humanize the ideals, without which civilization can become either sterile or self-destructive.

A. B. Pippard, *Reconciling Physics with Reality* (Cambridge U. P., Cambridge, 1972), p. 4.